Optimization and Engineering
https://doi.org/10.1007/s11081-023-09833-9

RESEARCH ARTICLE

Multi-objective structural optimization of vehicle wheels: a method for preliminary design

P. Stabile[1] · **F. Ballo**[1] · **M. Gobbi**[1] · **G. Previati**[1]

Received: 30 August 2022 / Revised: 26 July 2023 / Accepted: 2 August 2023

Abstract
The paper proposes an optimization procedure to be adopted by wheels design engineers for the identification of preliminary solutions to design lightweight and safe wheels. In particular, decisions related to the sizing of the wheel rim, to the number and type of spokes and to the spokes structural layout are addressed. The process relies on the combination of a simplified finite element model of the tire/wheel assembly and artificial neural networks used for global approximation, within a multi-objective optimization framework. Mass and compliance of the wheel are minimized at the same time, with constraints on structural safety and manufacturing. The method is applied to the preliminary design of the wheel of a lightweight electric vehicle specifically designed for energy efficiency competitions and allows to derive simple and general design guidelines for developing efficient products.

Keywords Wheel design · Multi-objective optimization · Structural optimization · Genetic algorithm · Neural networks

1 Introduction

The challenge of reducing the greenhouse gas (GHG) emissions of the road transport sector is continuously aiming at innovative and efficient design solutions.

Lightweight design offers the possibility for an environmentally friendly mobility. It is proved that mass reduction leads to a relevant decrease in energy consumption of road vehicles (Mastinu and Plöchl 2014; Stabile et al. 2021b). The wheels represent a large percentage of the rotational inertia of the vehicle and their effect on the vehicle

✉ M. Gobbi
massimiliano.gobbi@polimi.it

P. Stabile
pietro.stabile@polimi.it

[1] Via G. La Masa 1, 20158 Milan, Italy

Published online: 24 August 2023

energy consumption is relevant. The amount of energy required to accelerate rotating masses ranges between 1 and 2% of the total propulsion energy (Lee and Nelson 2005). Miller (2010) demonstrates that, for a mid-size hybrid electric vehicle, the inertia of rotating masses has an effect on fuel consumption similar to adding a passenger.

Inertial characteristics of the wheels also affect vehicle handling performance (Mastinu and Plöchl 2014; Gobbi and Mastinu 2001), being them a significant part of the unsprung mass of the vehicle. Lightweight design of wheels has therefore a positive effect on road holding.

Although mass minimization is a key feature, safety is another paramount requirement for wheels manufacturers. To ensure high safety standards, wheels are subject to severe and restrictive tests before production. As a consequence, a proper design of vehicle wheels has to guarantee adequate levels of structural stiffness and strength to comply with such strict constraints (Previati et al. 2019; Ballo et al. 2020a, b, 2016c, 2017).

Beside lightweight design and safety, aspects related to manufacturability and product style have to be considered by design engineers. Wheel design is often determined by tire size and by the space required by drivetrain and braking system. Most of wheels are made of aluminum alloy due to its lightweight characteristics and high manufacturability, which allows complex and fancy shapes. When it comes to customizing a vehicle, many consumers start with the wheels. For this reason, the aesthetic appeal greatly affects the design choices. When one thinks to new electric premium cars or SUVs (Sport Utility Vehicles), the role played by an appropriate and appealing wheel style in the succes of the vehicle appears immediately evident.

The design of vehicle wheels is therefore a complex and challenging task for engineers and many design variables have to be considered, such as number of spokes, spokes layout and connectivity, spokes shape and cross section dimensions. The large number and complexity of design aspects require a rigorous and efficient design method to support designers in taking the best decisions from the beginning of the process.

Structural multi-objective optimization techniques can be effectively employed for the optimal design of complex lightweight strucures, allowing a better final design and the reduction of design iterations and time (Ballo et al. 2021). Such techniques can be effectively applied to the design of wheels including lightweight, safety, manufacturability and aesthetic requirements. In the recent years, research in this field has increased significantly.

In the literature, structural and multi-objective optimization of wheels is a widely discussed topic. In several papers, topology optimization is employed for obtaining wheels with optimal material distribution for given sets of objectives and constraints. The optimal design is achieved using either gradient-based mathematical programming techniques such as SIMP (Solid Isotropic Material with Penalization) approach (Bendsoe and Sigmund 2004) or non-gradient based algorithms (Xie and Steven 1997; Deb and Goel 2002).

The work in Ballo et al. (2016b) exploits the SIMP method for the optimal design of a front motorcycle wheel. A minimum compliance problem is defined, with manufacturability-based constraints. To improve the accuracy of the optimization, the

force distribution acting at the tire/rim interface is computed through a simplified analytical model of the tire.

The SIMP-based topology optimization process performed by Das (2014) and Messana et al. (2018) aims to minimize the mass of the wheel while meeting design constraints related to safety and stiffness.

A heuristic approach based on the Bidirectional Evolutionary Structural Optimization (BESO) is exploited by Zuo et al. (2011) for the optimal topology design of a wheel. The work is aimed at maximizing the stiffness under volume and cyclical periodicity constraints.

Topology optimization is commonly acknowledged to be an effective tool to provide useful design guidelines to define an optimal wheel layout. However, it provides limited insights on aspects related to manufacturing and shape details. Such limitations mainly derive from the complexity of the results and low representation resolution (which is dependent on the element size). As a consequence, shape optimization is generally performed as a subsequent step to increase the level of details and to include actual manufacturing issues (Kim et al. 2022; Beigzadeh and Marzbanrad 2018). In these papers, integrated optimization methods, that combine topology and shape, are proposed. The topology optimization results provide the base design for the subsequent shape optimization, aimed at improving the initial design. The topology design space is the area filled by the spokes, while the shape optimization design parameters are related to the spokes geometry.

Given the large number and variety of design aspects in designing a wheel for road vehicles, multi-objective optimization approaches are also applied to enhance wheels structural and topological optimizations.

A multi-objective topology optimization method for the design of a steel wheel is proposed in Xiao et al. (2014), where the minimum compliance and the maximum fundamental eigenvalue are the two objectives.

In Zhang et al. (2021), a multi-objective topology optimization approach is applied to obtain the optimized layout of the wheel. The wheel is optimized under multiple load cases (radial, cornering and impact). Three design spaces are identified, namely the area between the hub and the rim, the rim well and the zone of the rim flanges.

A multi-objective optimization is applied in Wang et al. (2019) to the structural sizing optimization of a wheel. Mass and stresses occurring during impact loads are minimized by a Non-dominated Sorting Genetic Algorithm-II (NSGA-II). The design variables considered were related to the geometry and dimensions of the wheel rim, spokes and central hub.

The previously described wheels structural optimization approaches can be roughly divided into two strategies. In the first strategy, the topological optimization is applied to obtain a (almost) final geometry for the wheel complying with structural, space and symmetry constraints while minimizing one or more objective functions. Such geometry is refined by subsequent shape optimizations. In the second strategy, starting from a base wheel geometry, sizing and parametric structural optimizations are performed to increase wheel performances. Surrogate models are employed by some authors for the reduction of computational time.

In both cases, a relatively limited insight into the main geometrical features of the wheel is provided. Moreover, such methods are not really suitable for the early stage

design of the wheels, but mostly aim to provide a final geometry. The first stage of the design, however, is crucial as in this stage the basic choices that will influence all the design process are performed. Also, identifying at the very early stage the most promising design direction is cost and time effective, while late design changes are usually extremely expensive (Ashby 2011).

In this paper, a design approach especially conceived for the early stage design phase of wheels is proposed and applied to the design of the wheels of a ultra-efficient electric vehicle (Stabile et al. 2021b; Ballo et al. 2022; Shell 2022). The method differs from the previously described approaches as it aims to derive useful guidelines related to wheel topology (number of spokes and connectivity), spokes shape, dimensioning and sizing of the wheel rim and material. In particular, the method is able to handle the large number of design choices that have to be addressed in the early stage of the wheel design process. To this end, simplified numerical models and multi-objective optimization are employed.

The method is based on a preliminary study completed by the authors (2021). With respect to this preliminary study, in this paper the analysis is extended by including additional wheel layouts and geometries. A revised numerical model of the wheel rim is introduced, with the aim of having a more realistic representation of the structure of the rim. In order to obtain an optimized design that guarantees the manufacturability of the wheel rim, an additional optimization constraint taking into account the technological processes adopted to realize the part is included.

The paper is structured as follows: Sect. 2 briefly introduces the proposed design method; Sect. 3 presents the developed numerical model of the wheel, with reference to the finite element models of the tire and the wheel rim; in Sect. 4, the optimization algorithm is described; Sect. 5 reports the optimization results; in Sect. 6, differences between the proposed method and other design approaches are discussed. Finally, in Sect. 7, conclusions are given.

2 Design methodology

In this section the main steps of the proposed method for the early stage design of wheel rims are presented. The different steps are conceived in order to obtain a good compromise between computational time and accuracy of the solution. The method comprises the following steps:

- Definition of the appropriate load cases. Depending of the wheel type, different load cases should be considered in reference to the wheel application and to pertinent standards.
- Definition of the design variables. The design variables are related to rim and spokes. Rim shape is mostly constrained by the required profile to fit the tire, however, rim thickness can be changed and varied for different rim zones. For the spokes, number, base geometry and cross section can be considered. The geometry of the spokes can be traced back to a series of basic shapes to be combined in different ways to obtain a optimal structure. For any spoke geometry, different cross sections can be used to obtain different wheel performances. By changing

the base geometry and cross section of the spokes and optimizing the parameters of any combination, a clear understanding of the most convenient topology of the wheel can be obtained.
- Definition of the objective functions and of the constraints. On the basis of the pertinent load cases defined for the analysis, objective functions and constraints are defined.
- Simplified physical model of the tire. The tire model is used to have a good approximation of the forces that the tire transmits to the rim in the considered load cases. A correct estimation of the loads is of paramount importance for the correct definition of rim and spokes geometries with reference to stresses and deformations.
- Construction of the wheel model and global approximation. For each combination of shapes and design variables, a finite element analysis of the system should be performed to compute the values of objective functions and constraints. To reduce the computational time required for the exploration of the possible design combinations, a surrogate mathematical model of the system is obtained by using a neural network approximation.
- Computation of the Pareto optimal set. The trained neural networks are used to quickly compute the Pareto optimal set. For the solution of the non linear programming problem related to the computation of the set, a genetic algorithm is employed.
- Choice of the desired optimal solution and verification. Among the optimal solution, one or more solutions are chosen for the subsequent refined design of the wheel. Such solutions are simulated by using the physical model in order to validate the global approximation process.

Figure 1 outlines the architecture of the proposed method. In the next sections, the different steps are described taking the design of wheels for an ultra-efficient electric vehicle as reference case study.

3 Wheel physical model

The aim of the presented method is to identify the most promising geometry solutions for the wheel design. In the early stage of the design, a simplified geometrical representation of the wheel is sufficient for understanding the effects of the main parameters and spoke shapes. The physical model of the wheel, therefore, utilizes a simplified geometry both for the wheel rim and for the spokes. No detailed model of the connections between spokes and rim or wheel hub is considered. In the following, the physical model of the wheel is described. Particular attention is given to the estimation of the force transmitted by the tire to the rim.

3.1 Tire model

Finite Element modeling of the tire is conducted according to two main steps, as described in Korunovic et al. (2007), Ghoreishy (2006) and Yan (2003).

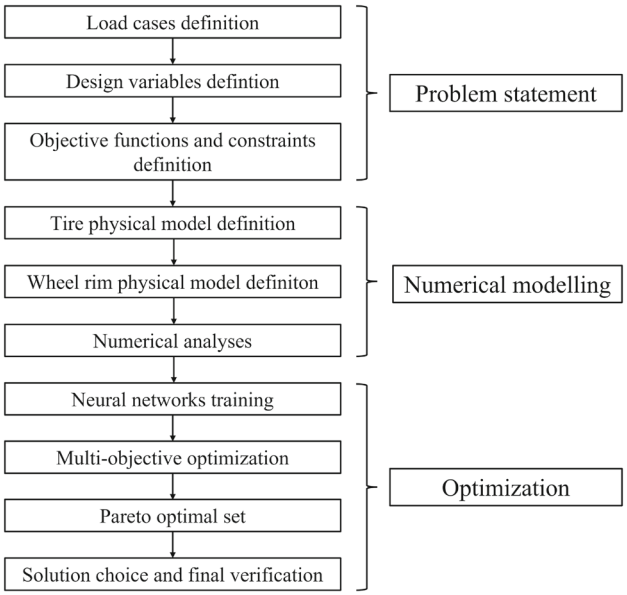

Fig. 1 Design method

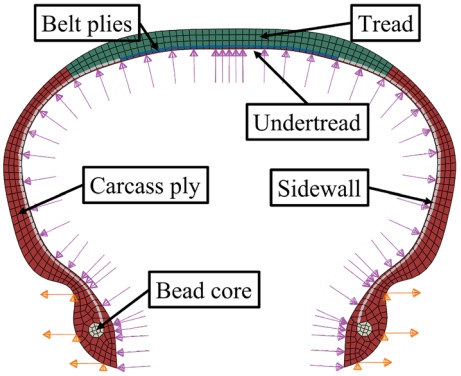

Fig. 2 Two-dimensional axisymmetric finite element model of the tire

In the first step, a two-dimensional axisymmetric finite element model of the tire is created. The geometry of the tire is digitally reconstructed from measurements on the actual tire with a FARO® measuring arm. Points located along the internal and external profile of the tire are sampled and used to reconstruct the actual geometry of the tire. The obtained shape is discretized by finite elements (Fig. 2). In the model, the main structural components that make up the tire (i.e. the tread, the sidewalls, the belts, the carcass ply and the beads) are included.

Steel belt plies and nylon carcass ply are modelled by equally spaced rebar layers (2014). The rubber components, namely tread, undertread and sidewalls are modelled as solid sections with isotropic hyperelastic materials described by a Neo-Hooke constitutive law (Ballo et al. 2016a).

Table 1 Radial and lateral stiffness obtained from experimental tests and numerical simulations for different inflating pressure values. Adapted from Stabile et al. (2021a)

Paratmeter	Inflating pressure (bar)	Experimental test (N/mm)	Numerical model (N/mm)
Radial stiffness	2.6	79	85
	3.6	120	130
	4.6	145	156
Lateral stiffness	2.6	40	36
	3.6	50	46
	4.6	58	53

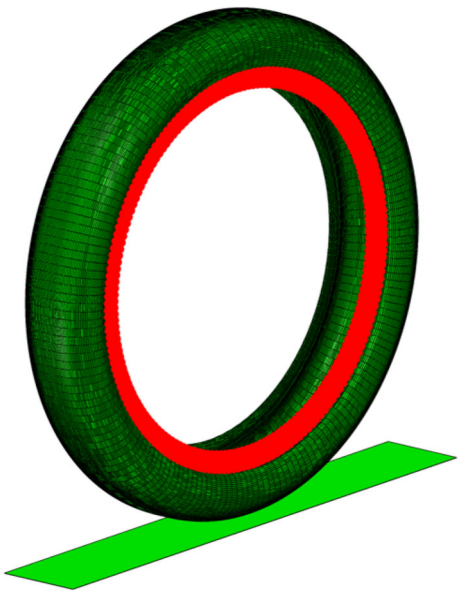

Fig. 3 3D finite element model of the 95/80 R16 tire studied

Due to the lack of information on the actual compound of the tire, the Neo-Hooke coefficients are identified from experimental static stiffness tests both in radial and lateral directions. A comprehensive description of the experimental tests performed for the identification of the tire parameters can be found in Stabile et al. (2021a). Stiffness values obtained from both experimental tests and numerical simulations are listed in Table 1.

The section of the tire is constrained at the bead seats region, where the tire is in contact with the rim. As the tire cross section was scanned with the tire off the rim, in the simulation the bead seats are laterally displaced to be exactly in the contact position. A uniform inflation pressure is applied at the inner surface as depicted in Fig. 2.

In the second step, a three-dimensional (3D) model is built by a complete revolution of the deformed section of the axisymmetric model. In this second step, the ground surface is modelled as a rigid plane as shown in Fig. 3. The contact between the tire and

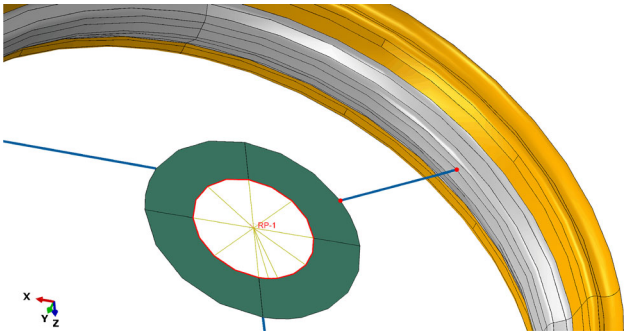

Fig. 4 Subdivision of the wheel rim FE model into three main regions

the plane is defined by a Coulomb friction model. Vertical and lateral loads are applied by imposing a displacement of the rigid plane. The reaction forces at constrained nodes are extracted by means of a handwritten Python script. Nodes for forces extraction are highlighted in red in Fig. 3.

The described modelling procedure allows to approximate the forces acting at the tire/rim interface in a more realistic way, since the load-carrying mechanism of the tire (i.e. how tire/terrain contact forces are transferred to the wheel rim) is simulated. Such an approach has the main advantage of decoupling the two models (i.e. the tire and the wheel rim), with a significant reduction of the computational time (Ballo et al. 2018). On the other hand, some simplifications are made, namely

- the simulation is static, tire rotation is neglected;
- interaction between tire and rim at the contact surface is neglected;
- effects of local stiffness of the rim on the transmitted tire forces are neglected.

The proposed simplified tire modelling approach has proved to be effective in providing an accurate stress field estimation on the wheel both for static (Ballo et al. 2016a, 2018) and dynamic (Ballo et al. 2020b; Previati et al. 2019) loading conditions.

3.2 Wheel rim model

The wheel rim numerical model is divided into three main regions, namely the outer rim, the central hub and the spokes.

The outer rim is modelled by means of three-dimensional shell elements that reproduce the rim profile. Two partitions identify three regions of the wheel outer rim, namely the rim well (gray area in Fig. 4) and the rim bead seats (orange area in Fig. 4). Each region features a different rim thickness.

Tire-rim reaction forces are introduced as a nodal force distribution applied at the bead seats.

The rim central hub is built as a three-dimensional shell. As shown in Fig. 5 , the offset between the mounting surface and the wheel central plane is reproduced. A kinematic coupling realizes the connection between the flange inner edge and a central node fixed to the ground (Fig. 4). Linear quadrilateral elements are used for the modelisation of both the outer rim and the central hub. The adoption of shell

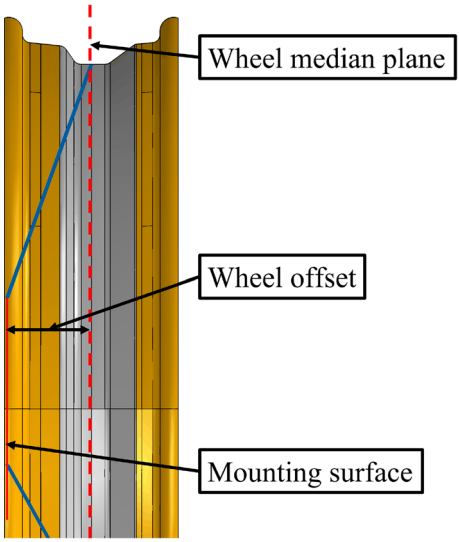

Fig. 5 Half section of the wheel rim FE model, with reference to the wheel offset

elements is justified by the fact that both the outer rim and the central hub feature the thickness much smaller than the other dimensions.

The spokes are modelled by linear beam elements (Fig. 4), connecting the outer nodes on the outer edge of the central hub and the portion of the rim surface connected to the spoke tip. Beam elements are exploited due to the significantly greater length dimension with respect to the other two dimensions. The connection between beams and shells is realized by sharing the nodes at the interface. The feasibility of modelling the wheel rim in such a way is demonstrated by performing comparative simulations on a numerical model where the outer rim is realized using solid elements. Displacements comparison between the two models shows satisfactory results, with maximum difference of approximately 1.5%.

The proposed simplified modelling approach allows an easy parametrization and management of a large variety of structural layouts and spokes cross sections, which enables the designer to identify one (or few) promising structural configurations at the very beginning of the design phase, when generally more degrees of freedom (i.e. more design variables) are left to the designer. On the other hand, such modelling approach comes with some simplifications, in particular, the stiffening effect introduced by the local geometry at the connection between the spoke and the wheel rim and hub is neglected. The other main simplification is that of underestimating the stress field at the rim-spoke and hub-spoke connections, which is mainly influenced by the notch effect given by the local geometry in those regions. It is clear that the two mentioned aspects need to be addressed in a subsequent refined design optimization stage, where also more details of the local geometry are defined by the wheel designer. In this phase, other critical aspects related to the safety of the wheel under static and fatigue loading conditions are considered (Ballo et al. 2016c, 2020a).

3.3 Load cases

The numerical model of the wheel allows to easily include several load cases in the simulation. Durability (fatigue life), impact resistance and structural stiffness are commonly assessed in the wheel design process.

As the wheel studied in this paper is designed to be mounted on a lightweight quadricycle for energy efficiency competitions, the structural stiffness is of paramount importance. Excessive wheel deformations, due to the loads that occur while the vehicle is running, can lead to additional power losses.

Buckling problem, which is typical of beam-columns and thin-walled plates, is used as criterion to asses the wheel failure mechanism. Loads in radial and lateral direction are applied to the wheel rim as described in Sect. 3.1.

In the present case, fatigue life and impact resistance are of secondary importance. In particular, the lightweight quadricycle on which the wheels are mounted is designed to have a limited service life. Moreover, the competition usually takes place on flat and smooth roads, without holes or critical obstacles to overcome.

If standard automotive wheels were considered, the proposed simplified numerical model of the tire/wheel assembly can be easily employed to simulate also fatigue and impact loading conditions in a preliminary design phase. With regards to durability, the procedure proposed in Ballo et al. (2020a) can be employed to simulate time varying loading. Load spectra of vertical and lateral force are applied to the tire physical model. Tire-rim reaction forces, extracted as described in Sect. 3.1 and representing the actual stress time history acting on the rim, are applied to the wheel rim physical model and moved along the bead seats region to simulate wheel rotation. Since the connection between spokes and outer rim is modeled in a simplified way, the obtained state of stress in these regions must be adjusted by means of appropriate corrective coefficients (Topaç et al. 2012; Pilkey 1997), so as to have a reasonable fatigue life assessment of the wheel rim.

For the impact resistance, simplified numerical approaches are presented in the literature. They have proven to be effective in simulating the wheel response in the case of impact test. In Shang et al. (2005), the simplified approach relies on a static analysis and a static equivalent load equal to 10 times the weight of the stricker is applied to simulate the impact effect of the dynamic loading. In Chauhan et al. (2015), the kinetic energy of the stricker is reduced by 20% to compensate for the absence of the tire in the simulation.

4 Multi-objective optimization algorithm

The design method follows a multi-objective optimization approach, where both the mass and compliance of the wheel are minimized at the same time.

Design variables include the wheel periodicity pattern, the topology (i.e. connectivity) and shape of the spokes and the rim thickness. Stiffness and safety (buckling) constraints are included in the optimization, as well as manufacturing constraints.

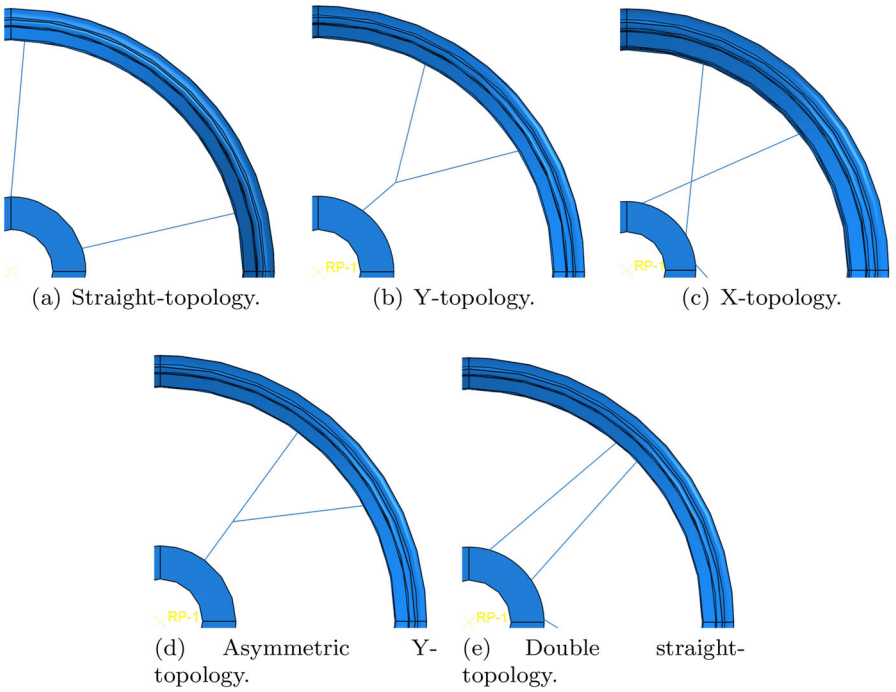

(a) Straight-topology. (b) Y-topology. (c) X-topology.

(d) Asymmetric Y-topology. (e) Double straight-topology.

Fig. 6 Spokes topologies considered in the optimization

4.1 Design variables

Design variables describe the main geometric features of the wheel. Wheels with 3, 5 and 7 spokes layout are considered in the optimization. Five distinct spoke topologies are investigated, namely: straight-shape (Fig. 6a), Y-shape (Fig. 6b), X-shape (Fig. 6c), asymmetric Y-shape (Fig. 6d) and double straight-shape (Fig. 6e), each one described by a dedicated set of parameters.

As regards the straight spokes, the only design variable is the spoke rotation angle (angle α in Fig. 7), namely the angle between the spoke and an axis passing through the hub center and the spoke root (see Fig. 7).

Concerning the spokes with Y-topology, two additional angles β and γ determine the location of the spoke-rim connection points and the position of the bifurcation point (see Fig. 8).

Likewise, for the X-topology, the angles β and γ define the position of the connection points with the hub and the rim respectively (see Fig. 9).

The asymmetric Y spoke has a structure divided into two parts. The main part is parameterized as a straight spoke while the two additional design variables k and δ determine the location of the bifurcation point and the orientation of the secondary member, as depicted in Fig. 10.

For the double straight-topology, the same design variables of the X-topology are used to define the four connection points of the spoke with the hub and rim.

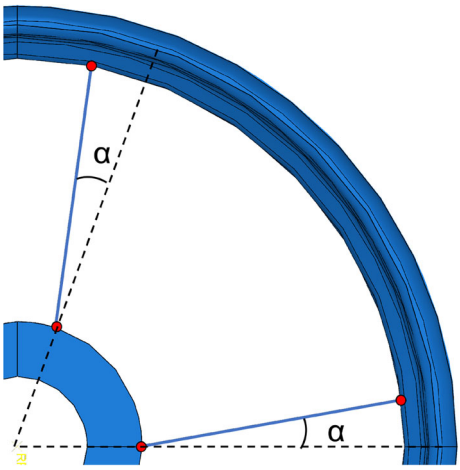

Fig. 7 Design variables related to the straight-topology of the spokes

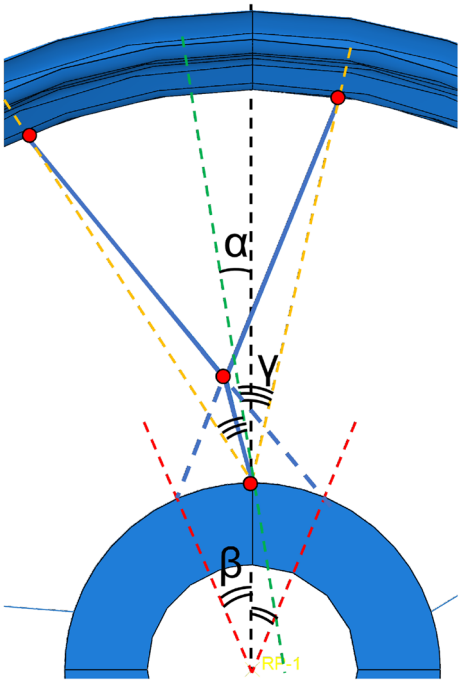

Fig. 8 Design variables related to the Y-topology of the spokes

Table 2 summarizes the design variables related to the spokes topology and their range.

For each topology, four different spokes cross sections are considered, namely rectangular, C-shaped, I-shaped and cross-shaped cross section. For each cross section, the set of design variables shown in Fig. 11 is considered. All the considered wheel structures have spokes with same type of section and dimensions, except for the structure

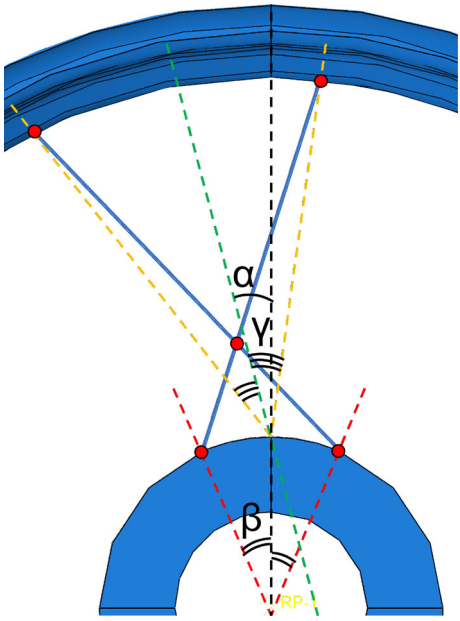

Fig. 9 Design variables related to the X-topology of the spokes

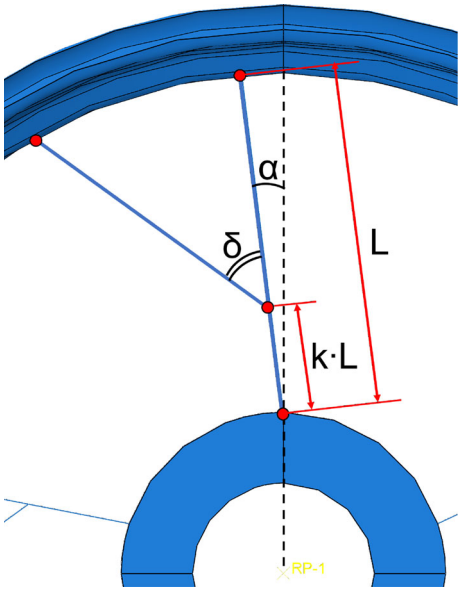

Fig. 10 Design variables related to the asymmetric Y-topology of the spokes

featuring asymmetric Y shaped spokes, which features cross sections with different size on the main and the secondary member.

The design variables that define the size of the spokes cross-section are listed in Table 3.

Table 2 Design variables related to the spokes topology

Topology	Design variable	Range
Straight	α	[0°; 31°]
Y	α	[0°; 31°]
	β	[16°; 23°]
	γ	[8°; 23°]
X	α	[0°; 31°]
	β	[16°; 23°]
	γ	[8°; 23°]
Asymmetric Y	α	[0°; 31°]
	k	[0.3; 0.8]
	δ	[16°; 47°]
Double-straight	α	[0°; 31°]
	β	[16°; 23°]
	γ	[8°; 23°]

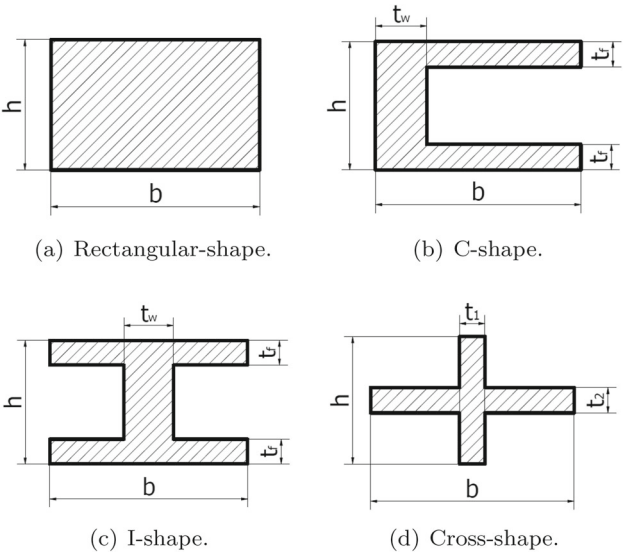

(a) Rectangular-shape. (b) C-shape.

(c) I-shape. (d) Cross-shape.

Fig. 11 Spokes cross-sections considered in the optimization

To ensure manufacturability, the width of the central hub is set to be equal to the width of the spokes.

Concerning the rim, two design variables are assigned: the thickness of the rim in the central region and the one in the regions of the bead seats (see Table 4).

Table 3 Design variables related to the spokes cross-sections

Section type	Design variable	Range
Rectangular	h	[5; 25.5 mm]
	b	[5; 87 mm]
C-shape	h	[5; 25.5 mm]
	b	[5; 87 mm]
	t_w	[1; 21.5 mm]
	t_f	[1; 42 mm]
I-shape	h	[5; 25.5 mm]
	b	[5; 87 mm]
	t_w	[8; 21.5 mm]
	t_f	[1; 42 mm]
Cross-shape	h	[5; 25.5 mm]
	b	[5; 87 mm]
	t_1	[1; 81 mm]
	t_2	[1; 21.5 mm]

Table 4 Design variables related to the rim sections

Rim section	Design variable	Range
Rim well	t_{well}	[1; 6 mm]
Rim bead seats	t_{bead}	[1; 6 mm]

4.2 Objective functions

For the design of the wheel for the ultra-efficient electric vehicle two objective functions are considered, namely wheel mass and compliance.

The compliance function is defined as

$$U(\mathbf{x}) = \frac{1}{2}\mathbf{u_s}^T[\mathbf{K}]\mathbf{u_s} + \frac{1}{2}\mathbf{u_c}^T[\mathbf{K}]\mathbf{u_c} \tag{1}$$

where U is the total strain energy, $[\mathbf{K}]$ is the global stiffness matrix, $\mathbf{x}$ is the vector of the design variables, $\mathbf{u_s}$ and $\mathbf{u_c}$ are the mean value of the nodal displacements during straight and cornering motion respectively. As shown in Eq. 1, the elastic strain energy U has two contributions: the first one refers to the straight motion of the vehicle, while the second contribution accounts for the cornering load case. In both cases, loads are applied in different portions of the rim circumference, with the aim of simulating the rolling motion of the wheel. An angular span equal to 36° is considered between two adjacent positions.

4.3 Constraints

Design constraints are related to the structural stiffness, to the safety and to the manufacturing of the wheel.

The first group of constraints is related to the structural stiffness of the wheel in radial, bending and torsional directions.

Radial stiffness is evaluated by applying a cosine radial force distribution on the bead seats of the rim, over an angular span of 60 degrees (Stearns et al. 2004, 2006; Raju et al. 2007). In this case, displacements and rotations of the central hub are constrained. The radial stiffness is defined as

$$K_{rad} = \frac{F_{rad}}{u_{rad}} \tag{2}$$

where F_{rad} is the resultant radial force and u_{rad} is the average radial displacement of the nodes located in the center of the loaded region. The radial stiffness is evaluated at three different angular locations of the wheel rim, namely the spoke centerline, the middle position between two adjacent spokes and an intermediate position not coinciding with one of the previous two locations. The term K_{rad} in Eq. 2 is the average value of the radial stiffnesses computed for the three considered loading positions.

To calculate bending and torsional stiffness, the rim is fixed at the rim flanges and a concentrated bending or torsional moment is applied at the central hub.

The second set of constraints refers to the safety of the wheel. Global buckling is evaluated by means of the eigenvalue problem of Eq. 3 (Cook et al. 2001)

$$([\mathbf{K}] + \lambda_b[\mathbf{K_\Theta}])\partial\mathbf{D} = \mathbf{0} \tag{3}$$

where $[\mathbf{K_\Theta}]$ is the stress stiffness matrix evaluated for stresses associated to the applied arbitrary load. The eigenvector $\mathbf{D}$ associated to the eigenvalue λ_b defines the shape of the critical deformed configuration. In the analysis, external loads are applied in different locations of the rim to account for the rolling motion of the wheel. The eigenvalue problem is solved by means of the Abaqus standard solver. The constraint on global buckling therefore reads

$$\lambda_b > \lambda_{b,cr} \tag{4}$$

In addition to Eq. 4, localized instabilities due to geometric features may occur as local buckling phenomenon. Such a condition is typical of thin-walled cross sections and is modeled through the simplified, but general, expression given by Ashby (2011)

$$\phi \leq \phi_{cr} \tag{5}$$

where ϕ is the shape efficiency factor of the beam cross section subject to elastic bending (Ashby 2011; Gobbi et al. 2017), defined as

$$\phi = \frac{12I}{A^2} \tag{6}$$

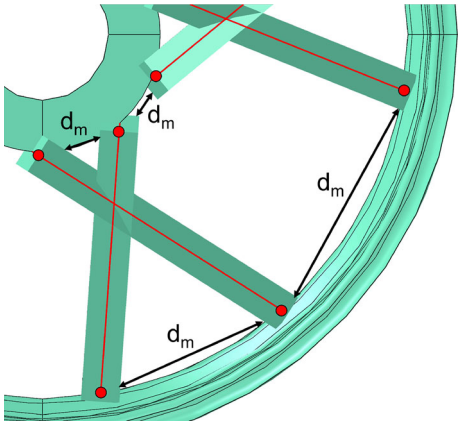

Fig. 12 Manufacturing constraint

Table 5 Design constraints limit values

Constraint	Parameter	Limit value
Radial stiffness	$K_{rad,cr}$	$2.8 \cdot 10^3$ N/mm
Lateral stiffness	$K_{bend,cr}$	$7 \cdot 10^4$ Nm/rad
Torsional stiffness	$K_{tors,cr}$	$7 \cdot 10^4$ Nm/rad
Global buckling	$\lambda_{b,cr}$	1
Local buckling	ϕ_{cr}	36.6
Manufacturability	$d_{m,cr}$	3 mm

where I and A are the second moment of inertia and the area of the cross section respectively. The critical value ϕ_{cr} of Eq. 5 depends on the cross section material and reads

$$\phi_{cr} \cong 2.3\sqrt{\frac{E}{\sigma_{adm}}} \tag{7}$$

where E and σ_{adm} are the Young Modulus and the admissible stress of the material respectively.

Finally, a third class of constraints takes into account the manufacturing phase of the wheel. In particular, milling and turning are considered as the main technological processes used for the construction of the wheel for a racing quadricycle. The manufacturing constraint aims at ensuring the feasibility of the part. A lower limit for the distance between the structural members of the spokes is set, as shown in Fig. 12for the X-spoke case.

Table 5summarizes the limit values of the design constraints.

4.4 Optimization formulation

The formulation of the optimization problem reads

$$\begin{aligned} \underset{\boldsymbol{x}}{\text{minimize}} \quad & \begin{pmatrix} m(\mathbf{x}) \\ U(\mathbf{x}) \end{pmatrix} \\ \text{subject to} \quad & K_{rad,cr} - K_{rad} \leq 0 \\ & K_{bend,cr} - K_{bend} \leq 0 \\ & K_{tors,cr} - K_{tors} \leq 0 \\ & 1 - \lambda_{cr} < 0 \\ & \phi - \phi_{cr} \leq 0 \\ & d_{m,cr} - d_m \leq 0 \\ \mathbf{x} \in \mathcal{X} \end{aligned} \tag{8}$$

The multi-objective optimization problem stated in Eq. 8 is solved by means of the Non-dominated Sorting Genetic Algorithm (NSGA) (Srinivas and Deb 1994).

The initial population is generated by applying a low-discrepancy Sobol sequence, to sample efficiently the design variable space. The dimension of the initial population is set equal to one thousand, so as to ensure a good compromise between uniformity of the distribution and fast computational time.

The fitness of each individual F_i is assigned according to his level of Pareto-optimality (i.e. the rank i) as

$$F_i = \frac{N_r - i + 1}{\sum_{j=1}^{N_r} (N_r - j + 1) \frac{N_{si}}{N}} \tag{9}$$

where N_r is the highest rank of the population, N_{si} is the number of individuals of rank i in the population and N is the population size.

Design constraints are introduced by means of a fitness penalization approach, i.e. a penalty that decreases the fitness is applied to unfeasible solutions. Hence, the fitness formulation reads

$$Fitness = F_i - \sum_{k=1}^{N_c} \frac{|C_{k,i} - C_{cr,k}|}{C_{cr,k}} \tag{10}$$

where N_c is the number of constraints, $C_{k,i}$ is the value of the k-th constraint for the i-th individual and $C_{cr,k}$ is the limit value of the k-th constraint (as defined in Table 5).

Sharing function approach (Goldberg and Richardson 1987) is employed to maintain an even distribution of solutions in the objective functions space during the optimization. A low fitness value is given to points with minimum distance relative to

other points, according to the function of Eq. 11

$$Sh(d_{ij}) = \begin{cases} 1 - \left(\frac{d_{ij}}{\sigma_{share}}\right)^{\epsilon} & if \quad d_{ij} \leq \sigma_{share} \\ 0 & otherwise \end{cases} \tag{11}$$

where d_{ij} is the distance between two individuals in the normalised objective functions space, σ_{share} and ϵ are two parameters set equal to 0.02 and 2 respectively (Mastinu et al. 2006).

The fitness function is adjusted as

$$\overline{Fitness} = \frac{Fitness}{\sum_{j=1}^{N} Sh(d_{ij})} \tag{12}$$

A single-point crossover is adopted for the reproduction stage. The crossover selection probability of each individual is based on the roulette wheel strategy (Holland 1992). A random mutation of the individuals is introduced in the algorithm, the probability of mutation is set equal to 1%.

5 Global approximation

The wheel finite element model presented in Sect. 3 allows to evaluate the responses for the design constraints and for the objective functions. The average simulation time for the model to run is about 90 s. Genetic algorithms require both a large population of individuals and a large number of iterations to ensure the algorithm convergence. To avoid the excessive increase in computational time, global approximation techniques are used. The physical model is substituted by another purely mathematical model which is able to give computational results very quickly.

In particular, the multi-layer perceptron neural network (Hertz et al. 1991; Haykin 1998) is employed as approximation tool to compute response values for the objective functions and the constraints. A set of neural networks is trained for each topology of wheel analyzed, namely for each shape and cross-section of the spokes taken into account. The number of spokes is treated as a design variable in the trainig process. Design variables number ranges from 8 (in the simplest case, i.e. the straight spokes with rectangular section layout) to 16 (more complex cases).

The training set consists of six thousand samples extracted from a Sobol sequence covering the entire design space. Each sample is simulated by the physical model to get the structural responses.

The typical structure of the proposed ANNs features a single hidden layer with 12 neurons, that allows to approximate the values of the compliance function and structural stiffness of the wheel with a high level of accuracy. Only for the approximation of the critical buckling factor, given the non-linearity of the function, a second hidden layer with 6 neurons is added. A hyperbolic tangent function is used as activation function of the hidden layers neurons. The number of neurons in the hidden layers and the share of data allocated for training and validation are set following a trial-and-error

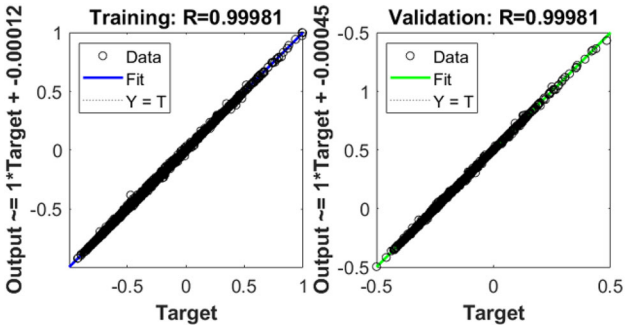

Fig. 13 Neural network training regression for the global buckling constraint. Plots refer to the X-topology with C-shape cross section wheels layout

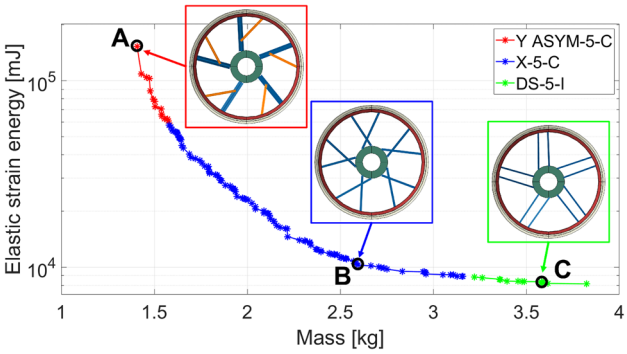

Fig. 14 Pareto optimal set in the objective functions domain. The wheels in the boxes show the structural layout of the highlighted solutions A, B and C

process aimed at decreasing the approximation error. More precisely, 75% of the set is used for training, the remaining part is employed to check the generalization capabilities of the network. Bayesian regularization (Burden and Winkler 2009; Neal 2012) is adopted to increase the robustness of the global approximation and avoid overtraining.

Regression plots are shown in Fig. 13, for the outputs related to the global buckling constraint.

6 Results

Optimization runs have been performed for each wheel structural configuration. Then, all the Pareto optimal solutions obtained from each optimization run have been compared to identify the most promising structural configurations.

The final Pareto optimal set is derived from the superimposition of the Pareto optimal sets of all the investigated structural configurations. The semi-log plot of the final Pareto optimal set in the objective functions domain is given in Fig. 14.

Wheels with a 5-spokes periodicity seem to be the optimal solution for obtaining lightweight and stiff wheels. As shown in Fig. 14, the Pareto frontier is made

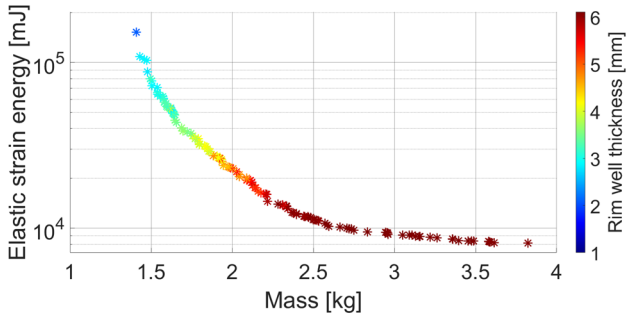

(a) Rim thickness constraint.

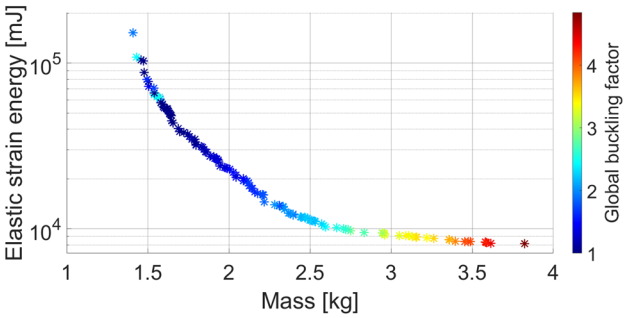

(b) Global buckling constraint.

Fig. 15 Representation of the design constraints trend for the Pareto optimal set

by different topologies and shapes. Wheels with higher stiffness feature the double straight-spokes topology and I-shape cross-section. Moving along the Pareto front, towards less stiff but lighter solutions, wheels are characterized by spokes with X-topology and C-section. Finally, the asymmetric Y-topology is the most suitable layout for extremely lightweight wheels.

Other interesting considerations can be deducted from Fig. 15, which shows the values of the rim thickness and the buckling safety factor of the obtained Pareto-optimal solutions. In particular, from Fig. 15a it emerges that solutions with low compliance feature a rim with the highest possible thickness. Moving towards lighter solutions, the limiting constraint is the one the buckling safety factor (Fig. 15b).

To check the accuracy of the neural networks, the performances of the three solutions highlighted in Fig. 14 have been computed by means of the physical model. Results of the comparison are summarized in Table 6 and show errors below 1% for all the computed objective function and constraints. Slightly higher differences have been found for the global buckling constraint, with a maximum error equal of 1.4%. However, the critical buckling load factor computed by the ANNs is lower than the one obtained from the physical model, ensuring a conservative approach.

Table 6 Percentage difference between responses approximated by the neural networks and computed by the physical model on the three optimal solutions of Fig. 14

Response	A (%)	B (%)	C (%)
Elastic strain energy	0.3	0.4	0.1
Radial stiffness	0.5	0.4	0.5
Bending stiffness	0.4	0.6	1
Torsional stiffness	1	0.7	1.2
Global buckling	1.4	1.2	0.9

7 Discussion

The implemented methodology has proved to be effective in providing important guidelines in the early stages of the wheel design process.

Differently from current state of the art design procedures based on topology optimization, the proposed method provides the designers with a broader vision of the critical parameters involved in the design of lightweight and safe wheels. As shown by the case study discussed in the paper, the presented method allows to determine, in addition to the topology of the spoke (number and connectivity), also shape of the spoke and size of the rim. Obviously, such an advantage comes with the drawback of introducing additional simplifications in the numerical modeling of the wheel, which is fully justified in a preliminary design stage. Therefore, the proposed method is not meant as an alternative to topology and shape optimization approaches, rather it offers an additional support to be employed in the conceptual phase for deriving simple and general design rules encountering the largest number of aspects related to wheel design.

The "modular" approach of the design methodology allows to easily include additional load cases, new layouts and shapes in the algorithm. In fact, the physical model of the wheel rim is extremely simplified and any kind of spoke topology can be parameterized in a straightforward way.

Once the physical model is built, it can be used to train the ANNs to be used in the optimization phase. Trained ANNs can be collected in a single database and can be reused for wheels that share similar features (e.g. same rim and hub, same tire size, etc.) and this database can be continuously updated when new layouts/shapes need to be investigated.

8 Conclusion

In the paper, an optimization approach suitable for the design of vehicle wheels is presented. The proposed method aims to provide design engineers with preliminary solutions and guidelines, taking into account the number of design criteria that characterize the design of vehicle wheels (e.g. lightweight, safety, manufacturability and aesthetics).

In order to have an effective representation of the forces acting on the wheel rim, finite element-based models of tire and wheel rim are developed. The tire numerical

model aims to reproduce the actual geometry and structural properties of the studied tire. Tire/rim interface reaction forces are numerically computed and applied as nodal force distributions to the rim.

A multi-objective optimization method is employed to optimize the wheel structural layout for minimum mass and minimum compliance. Design parameters allow to define the optimal number, topology and cross-section of the spokes, size of the rim and the spokes. Constraints related to wheel safety, structural stiffness and manufacturability are considered. A Non-dominated Sorting Genetic Algorithm (NSGA) is adopted for obtaining the Pareto optimal set of wheel designs.

To reduce the computational effort, the numerical model of the wheel is exploited to train a set of Artificial Neural Networks (ANNs) for each spoke topology and cross-section considered. Hence, a collection of ANNs is implemented and employed by the optimization algorithm for approximating objective functions and constraints.

Direct comparison among the obtained Pareto optimal set for all the considered structural configurations allowed to identify the most promising solutions. In particular, results showed that lightweight and stiff wheels design can be achieved through a 5-spokes layout. The Pareto front is composed by the combination of three spokes structural layouts, namely spokes with double straight-shape, X-shape and asymmetric Y-shape. Spokes featuring double straight-shape layout and I-cross section have to be selected to obtain low compliance wheels. If solutions with low mass are desired, spokes designs with asymmetric Y-shape and C-cross section are preferred.

The obtained results show that Pareto-optimal solutions with lower compliance feature an outer wheel rim with maximum allowable thickness, while solutions with higher compliance (and lower mass) lay on the constraint of global buckling.

Funding Open access funding provided by Politecnico di Milano within the CRUI-CARE Agreement.

Declarations

Conflict of interest The authors declare that they have no conflict of interest.

References

ABAQUS/Standard User's Manual (2014) Version 6.14, United States

Ashby MF (2011) Chapter 5—Materials selection-the basics. In: Ashby MF (ed) Materials selection in mechanical design, 4th edn. Butterworth-Heinemann, Oxford, pp 97–124. https://doi.org/10.1016/B978-1-85617-663-7.00005-9

Ballo F, Gobbi M, Mastinu G, Previati G (2016) Motorcycle tire modeling for the study of tire-rim interaction. J Mech Des 138:51404–51413. https://doi.org/10.1115/1.4032470

Ballo F, Previati G, Gobbi M, Mastinu G (2018) Tire-Rim interaction, a semi-analytical tire model. J Mech Des Trans ASME 140(4):041401. https://doi.org/10.1115/1.4038927
Ballo F, Previati G, Mastinu G, Comolli F (2020) Impact tests of wheels of road vehicles: a comprehensive method for numerical simulation. Int J Impact Eng 146:103719
Ballo FM, Gobbi M, Mastinu G, Previati G (2021) Optimal lightweight construction principles. Springer, New York. https://doi.org/10.1007/978-3-030-60835-4
Ballo F, Stabile P, Gobbi M, Mastinu G (2022) A lightweight ultra-efficient electric vehicle—multi-physics modeling and driving strategy optimization. IEEE Trans Veh Technol XX:1. https://doi.org/10.1109/TVT.2022.3172174
Ballo F, Frizzi R, Gobbi M, Mastinu G, Previati G, Sorlini C (2017) Numerical and experimental study of radial impact test of an aluminum wheel—towards industry 4.0 virtual process assessment. In: Proceedings of the ASME 2017 international design engineering technical conferences and computers and information in engineering conference, Cleveland, Ohio, USA, pp 1–10. https://doi.org/10.1115/DETC2017-67703
Ballo F, Mastinu G, Gobbi M (2016b) Lightweight design of a racing motorcycle wheel. In: SAE 2016 world congress and exhibition. SAE International. https://doi.org/10.4271/2016-01-1576
Ballo F, Mastinu G, Previati G, Frizzi R, Mastroberti D, Sorlini C (2016c) Lightweight design and construction of aluminum wheels. In: SAE 2016 world congress and exhibition. SAE International. https://doi.org/10.4271/2016-01-1575
Ballo F, Mastinu G, Previati G, Gobbi M (2020a) Numerical modelling of the biaxial fatigue test of aluminium wheels. In: Proceedings of the ASME design engineering technical conference. American Society of Mechanical Engineers (ASME), St. Louis, vol 4. https://doi.org/10.1115/DETC2020-22142
Beigzadeh S, Marzbanrad J (2018) Automotive wheel optimization to enhance the fatigue life. Autom Sci Eng. https://doi.org/10.22068/ijae.8.3.2739
Bendsoe MP, Sigmund O (2004) Topology optimization: theory, methods and applications. Springer, New York
Burden F, Winkler D (2009) Bayesian regularization of neural networks. Humana Press, Totowa, pp 23–42. https://doi.org/10.1007/978-1-60327-101-1_3
Chauhan MR, Kotwal G, Majge A (2015) Numerical simulation of tire and wheel assembly impact test using finite element method. In: Symposium on international automotive technology 2015. SAE International. https://doi.org/10.4271/2015-26-0186
Cook RD, Malkus DS, Plesha ME, Witt RJ (2001) Concepts and applications of finite element analysis, 4th edn. Wiley, New York
Das S (2014) Design and weight optimization of aluminum alloy wheel. Int J Sci Res 4:1–12. https://doi.org/10.29322/ijspr
Deb K, Goel T (2002) Multi-objective evolutionary algorithms for engineering shape design. Springer, Boston, pp 147–175. https://doi.org/10.1007/0-306-48041-7_6
Ghoreishy MHR (2006) Finite element analysis of the steel-belted radial tyre with tread pattern under contact load. Iran Polym J (Engl Ed) 15:667–674
Gobbi M, Mastinu G (2001) Analytical description and optimization of the dynamic behaviour of passively suspended road vehicles. J Sound Vib 245:457–481. https://doi.org/10.1006/jsvi.2001.3591
Gobbi M, Previati G, Ballo F, Mastinu G (2017) Bending of beams of arbitrary cross sections—optimal design by analytical formulae. Struct Multidiscip Optim 5:5. https://doi.org/10.1007/s00158-016-1539-6
Goldberg DE, Richardson J (1987) Genetic algorithms with sharing for multimodal function optimization. In: Proceedings of the second international conference on genetic algorithms on genetic algorithms and their application. L. Erlbaum Associates Inc., pp 41–49
Haykin S (1998) Neural networks: a comprehensive foundation, 2nd edn. Prentice-Hall, Hoboken
Hertz JA, Krogh AS, Palmer RG (1991) Introduction to the theory of neural computation. Addison-Wesley, Boston
Holland JH (1992) Reproductive plans and genetic operators. MIT Press, Cambrige, pp 89–120
Kim J, Kim JJ, Jang IG (2022) Integrated topology and shape optimization of the five-spoke steel wheel to improve the natural frequency. Struct Multidiscip Optim. https://doi.org/10.1007/s00158-022-03183-3
Korunovic N, Trajanovic M, Stojkovic M (2007) Fea of tyres subjected to static loading. J Serb Soc Comput Mech 1:87–98

Lee J, Nelson D (2005) Rotating inertia impact on propulsion and regenerative braking for electric motor driven vehicles. In: 2005 IEEE vehicle power and propulsion conference, p 7. https://doi.org/10.1109/VPPC.2005.1554575

Mastinu G, Plöchl M (2014) Road and off-road vehicle system dynamic handbook. CRC Press, Boca Raton

Mastinu G, Gobbi M, Miano C (2006) Optimal design of complex mechanical systems: with applications to vehicle engineering. Springer, Berlin, pp 99–118. https://doi.org/10.1007/978-3-540-34355-4_4

Messana A, Sisca L, Getti C, Malvindi A, Ferraris A, Airale A, Carello M (2018) Design, optimization and production of aluminum alloy rim for the vehicle prototype idrakronos. In: CAD'18 proceedings. CAD Solutions LLC, pp 112–116. https://doi.org/10.14733/cadconfP.2018.112-116

Miller J (2010) Propulsion systems for hybrid vehicles, 2nd edn. The Institution of Engineering and Technology, London

Neal RM (2012) Bayesian learning for neural networks, vol 118. Springer, New York

Pilkey WD (1997) Peterson's stress concentration factors, 2nd edn. Wiley, New York

Previati G, Ballo F, Gobbi M, Mastinu G (2019) Radial impact test of aluminium wheels-Numerical simulation and experimental validation. Int J Impact Eng 126(November 2018):117–134. https://doi.org/10.1016/J.IJIMPENG.2018.12.002

Raju P, Satyanarayana B, Ramji K, Babu K (2007) Evaluation of fatigue life of aluminum alloy wheels under radial loads. Eng Fail Anal 14:791–800. https://doi.org/10.1016/j.engfailanal.2006.11.028

Shang R, Altenhof W, Li N, Hu H (2005) Wheel impact performance with consideration of material inhomogeneity and a simplified approach for modeling. Int J Crashworthiness 10(2):137–150. https://doi.org/10.1533/ijcr.2005.0333

Shell (2022) Shell eco-marathon. https://www.makethefuture.shell/en-gb/shell-eco-marathon. Accessed 23 Aug 2022

Srinivas N, Deb K (1994) Muiltiobjective optimization using nondominated sorting in genetic algorithms. Evol Comput 2(3):221–248. https://doi.org/10.1162/evco.1994.2.3.221

Stabile P, Ballo F, Mastinu G, Gobbi M (2021) An ultra-efficient lightweight electric vehicle-power demand analysis to enable lightweight construction. Energies. https://doi.org/10.3390/en14030766

Stabile P, Ballo F, Gobbi M, Previati G (2021) Multi-objective structural optimization of vehicle wheels. In: International design engineering technical conferences and computers and information in engineering conference. https://doi.org/10.1115/DETC2021-71062

Stabile P, Ballo F, Gobbi M, Previati G (2021a) Multi-objective structural optimization of vehicle wheels. In: International design engineering technical conferences and computers and information in engineering conference, volume 1: 23rd international conference on advanced vehicle technologies (AVT). https://doi.org/10.1115/DETC2021-71062

Stearns J, Srivatsan T, Prakash A, Lam P (2004) Modeling the mechanical response of an aluminum alloy automotive rim. Mater Sci Eng A Struct Mater 366:262–268. https://doi.org/10.1016/j.msea.2003.08.017

Stearns J, Srivatsan T, Gao X, Lam P (2006) Understanding the influence of pressure and radial loads on stress and displacement response of a rotating body: the automobile wheel. Int J Rotat Mach. https://doi.org/10.1155/IJRM/2006/60193

Topaç M, Ercan S, Kuralay N (2012) Fatigue life prediction of a heavy vehicle steel wheel under radial loads by using finite element analysis. Eng Fail Anal 20:67–79. https://doi.org/10.1016/j.engfailanal.2011.10.007

Tyre E, Organisation RT (2020) Standards manual 2020

Wang D, Zhang S, Xu W (2019) Multi-objective optimization design of wheel based on the performance of 13° and 90° impact tests. Int J Crashworthiness 24:1–26. https://doi.org/10.1080/13588265.2018.1451229

Xiao D, Zhang H, Liu X, He T, Shan Y (2014) Novel steel wheel design based on multi-objective topology optimization. J Mech Sci Technol 28:1007–1016. https://doi.org/10.1007/s12206-013-1174-8

Xie YM, Steven GP (1997) Basic evolutionary structural optimization. Springer, London, pp 12–29. https://doi.org/10.1007/978-1-4471-0985-3_2

Yan X (2003) Nonlinear three-dimensional finite element analysis of steady rolling radial tires. J Reinf Plast Compos 22(8):733–750. https://doi.org/10.1177/0731684403022008004

Zhang Y, Shan Y, Liu X, He T (2021) An integrated multi-objective topology optimization method for automobile wheels made of lightweight materials. Struct Multidiscip Optim 64:1–21. https://doi.org/10.1007/s00158-021-02913-3

Zuo Z, Xie Y, Huang X (2011) Reinventing the wheel. J Mech Des 133:024502-1. https://doi.org/10.1115/1.4003411